Robust control system development for VTOL-to-fixed wing flight transition with the EcoSoar UAV

A thesis in Automatic Control

Robert Hedman

September 6, 2019

A thesis presented for the degree of
Masters of Science / Civil Engineer

Department of Computer Science, Electrical and Space Engineering
Luleå University of Technology
Supervisors: K. Atta, K. Kochersberger
Examinator: G. Nikolakopoulos

Abstract

This is wehere we write about the abstract. asdasdasd asd asdasdjhsdkjhdsak dikd sdoj asodj asdoja sdojas do

Acknowledgements

Thank teachers that helped, Mr. K, Avory, Wife, etc.

[Lets see if they require rent before adding below]

I also want to extend a very warm thank you to Montford Special Needs College in Malawi for allowing me to stay there together with my wife during this thesis. The staff also provided all the support needed to become integrated with the local culture and helping out with practical issues such as getting a car, finding the hospital and providing a safe circle of friends.

Contents

1 List of variables

L_L	Lift from left wing
L_R	Lift from right wing
D_L	Drag from left wing
D_R	Drag from right wing
F_L	Lift due to aileron deflection, left side, outside propeller wake
F_{L_T}	Lift due to aileron deflection, left side, inside propeller wake
F_R	Lift due to aileron deflection, right side, outside propeller wake
F_{R_T}	Lift due to aileron deflection, right side, inside propeller wake
D_{α_L}	Drag due to aileron deflection, left side, outside propeller wake
$D_{\alpha_{L,T}}$	Drag due to aileron deflection, left side, inside propeller wake
D_{α_R}	Drag due to aileron deflection, right side, outside propeller wake
$D_{\alpha_{R,T}}$	Drag due to aileron deflection, right side, inside propeller wake
L_{W_L}	Lift from left winglet
L_{W_R}	Lift from right winglet
D_{W_L}	Drag from left winglet
D_{W_R}	Drag from right winglet
S_a	Surface area of one aileron, parts outside propeller wake
S_{a_w}	Surface area of one aileron, area inside propeller wake
c.g.	center of gravity (point)
T_L	Thrust from left propeller
T_R	Thrust from right propeller
S_w	Area of one wing, area outside of propeller wake
S_{w_w}	Area of one wing, area inside propeller wake
S_W	Area of one winglet
x_f	distance in x from c.g. to aileron force
x_T	distance in x from c.g. to thrust force
x_{ac}	distance in x from c.g. to wing aerodynamic center
x_W	distance in x from c.g. to winglet force
y_T	distance in y from c.g. to thrust force
y_f	distance in y from c.g. to aileron force
y_{ac}	distance in y from c.g. to wing aerodynamic center
y_w	width of propeller wake
b	wingspan
z_W	distance in z from c.g. to winglet force

2 Background

Virginia Tech, a University in Virginia, USA, has developed a fixed wing drone called the EcoSoar; a flying wing. It is an aircraft designed for fabrication, operation and maintenance in low- resource environments. The total cost of one EcoSoar is only around 350 USD when costs for all tools and materials have been accounted for and spread over ten aircraft.

EcoSoar has been successfully flown in Malawi at the test corridor established by UNICEF in Kasungu, where a simulated payload of dried blood spot samples (used for HIV testing) was delivered 19 km from a remote health clinic to the Kasungu airport. The aircraft is constructed of poster-board and 3D printed parts, making it easy to source in Malawi and low cost to repair if damaged.

Many flight operations occurring in Africa are converging on hybrid aircraft designs where the aircraft functions as a quadcopter in takeoff and landing but is capable of higher speed flight in a fixed wing configuration.

EcoSoar can currently be launched with a big bungee-cord or with a custom built launcher. It thus needs a field to both take off and land in since it can only land on its belly similar to that of any normal aircraft. Modifying the EcoSoar to have two engines, one on the front of each wing, instead of the current design of having one at the back, might allow it to hover, take off and land vertically eliminating the need for a launching system as well as the requirement of a big field for take-off and landing. It also eleiminates the risk of high speed crashes at launch due to a badly calibrated aircraft.

Adding VTOL capacity to this drone would greatly increase its range of possible missions and thus help humanitarian efforts centered around EcoSoar in Malawi.

To achieve VTOL not only is hardware modifications necessary but also a new control scheme is necessary.

2.1 EcoSoar hardware

The EcoSoar frame is mostly built out of 3D printed parts for the body and spars. The outer layer of the wings are made out of poster board and packing tape. Small micro servos actuate on the Elevons for control. The on board electronics include a flight computer (Pixhawk 1), any compatible receiver, an ESC (Electronic Speed Controller) for the brushless motor powering the propeller, a telemetry module with antenna and a gps module.

3 Problem Forumulation

This thesis will attempt to solve the problem of mathematically modeling the EcoSoar, develop a VTOL capable model based controller that can handle both hovering, transitioning into flying and flying, and finally implement the controller on the Pixhawk controller onboard the aircraft.

4 Theory

To develop this controller some basic concepts are required.

4.1 State Space

Many systems can be written as a set of differential equation.

Physical systems may sometimes be mathematically modeled by state space representation, given that it can be written on the same form as equation 1 below.

$$\dot{\bar{x}} = f(\bar{x}) + g(\bar{u}, \bar{x}) \tag{1}$$

The states, $\bar{x}$ are related by a set of first order differential equations and some input.

Systems can have one input and one state/output, called Single Input Single Output (SISO), or have either multiple input or outputs or both; Multiple Input Multiple Output (MIMO) systems.

A system with several states, i.e. $\bar{x}$ being a vector, and several inputs, i.e. $\bar{u}$ being a vector is thus represented by a set of functions $\bar{f}$ and $\bar{g}$.

From basic fundamental physical laws, e.g. newtons laws, a set of differential equation for many physical systems can be derived. Once the state space equations are known simulating the system is only a matter of choosing a differential equation solver. Simulink has built in solver for these equations over time making it easy to simulate the system once the equations are known.

4.2 State estimation/observers

A full state vector may not always be exactly measurable so estimating it is of importance. The Pixhawk PX4 firmware already includes an extended Kalman filter for estimating the position and attitude from an angular rate sensor, accelerometer, barometer and magnetometer. For this project the built in Kalman filter will be used to estimate the state with which the control system will act upon.

4.3 Reference Frames

When working with rigid bodies in 3d space a reference system is needed. In most of airplane dynamics for small scale aircraft the standard is a cartesian coordinate system with the x-axis aligned with North, y-axis aligned with East and the z-axis pointing down. The body frame is similar, x-axis pointing forwards, y-axis along right wing and z-axis through the belly of the aircraft, i.e. down when flying normally. This correspond to the well used Roll-Pitch-Yaw system.[3]

4.4 Quaternions

Euler angles are intuitive but suffer from singularities. Since normal aircraft normally do not spend time pointing straight up these singularities do not matter too much, but a VTOL capable tail-sitter will, so using quaternions is beneficial.

A quaternion, $\mathbf{q}$ is a four dimensional hyper complex number.[4]

$$\mathbf{q} = q_0 + q_1\mathbf{i} + q_2\mathbf{j} + q_3\mathbf{k} \tag{2}$$

where $i^2 = j^2 = k^2 = ijk = -1$.[6] The imaginary part can be referenced to as the vector part and q_0 the scalar part. The conjugate of a quaternion is defined as

$$\mathbf{q}^* = q_0 - q_1\mathbf{i} - q_2\mathbf{j} - q_3\mathbf{k} \tag{3}$$

The quaternion can also be represented as a vector:

$$\mathbf{q} = \begin{bmatrix} q_0 & q_1 & q_2 & q_3 \end{bmatrix} \tag{4}$$

The norm of a quaternion is defined by

$$||\mathbf{q}|| = \sqrt{\mathbf{q} \otimes \mathbf{q}^*} = \sqrt{q_0^2 + q_1^2 + q_2^2 + q_3^2} \tag{5}$$

If the norm of a quaternion is equal to 1 it is a unit quaternion. Unit quaternions are very computationally efficient at describing rotations in 3D. They also do not suffer from any singularities like the common Roll-Pitch-Yaw / Euler angles system. Unit quaternions can always be written as

$$\mathbf{q} = \begin{bmatrix} cos\theta \\ \mathbf{u}sin\theta \end{bmatrix} \tag{6}$$

where $\mathbf{u}$ is the vector $\begin{bmatrix} q_1 & q_2 & q_3 \end{bmatrix}$ describing the axis of which to rotate around and θ is proportional to the amount of rotation about that axis. Multiplying unit quaternions yield a unit quaternion describing the joint rotation of the two initial quaternions. The conjugate of a quaternion gives the opposite rotation direction around the same vector. This can correspond to going from a world frame to body frame, or vice versa. Multiplying a reference quaternion describing a set orientation for an object in 3D with the conjugate of its actual quaternion therefore gives the error in orientation, attitude.

A more in depth description of quaternions and their mathematics please see [6].

4.5 Equations of Motion, in body frame

4.6 Basic aerodynamics

When a wing moves through air two major forces act upon it, a lifting force and a drag force. The lift is primarily due to camber (the non symmetry of the cross section of the wing) and to the angle of attack: the angle at which the incoming air hits the wing. The same goes for drag.

- Bernoulli Equation, center of Pressure, etc
- Basic plate theory
- Aerodynamic center
- Aerodynamic forces and Moments
  - Lift, and moment, due to camber
  - Lift due to angle of attack
  - Drag
  - Forces/Moments due to airflow over Ailerons and Elevators
  - Forces and Moments due to sideslip and roll
  - Forces/Moment due to roll rate, pitch rate and yaw rate
- Propeller efficiency, airspeed, wake velocity

5 Mathematical Model of EcoSoar

5.1 Assumptions

- There is no external wind and so v_∞ is replaced with v which is the aircrafts velocity through the air.
- All forces operate on points in the $x-y$ plane, i.e. no offset in the z-direction (with the notable exception of the winglet forces). Forces may still have a z-component though.
- The propeller wake is unaffected by aircraft velocity, i.e. only determined by propeller speed.
- Airflow outside of wake is only determined by aircraft velocity.
- The aerodynamic centre (a.c.) is static and does not move with changes in speed and pressure. The moment around it, however, will vary and thus account for the effects of the a.c. movement.
- Airflow speed in wake is proportional to propeller rotational speed, $v_w = b_w\omega_i$, where b_w is a constant.
- The principal moments axis align with the symmetry plane; only diagonal elements in the inertia matrix aligned with the body frame coordinate axis.
- Roll moment due to sideslip angle, negligible due to lack of tail with verical offset from c.g.
- Yawing moment due to roll rate is negligible due to the lack of a tail.
- Forces and moments due to acceleration are not explicitly calculated; they are already included in dynamic model since it is based on forces.

5.2 Aircraft force diagram

The aircraft in question is the EcoSoar; a flying wing. It has two control surfaces, one on each wing called elevons. In front of each wing a motor and propeller is mounted providing thrust. The motors also supply an airflow over the control surfaces when the aircraft is not moving through the air.

The elevon forces, F_L, F_{L_T}, D_{a_L} and $D_{a_{L,T}}$, have only been marked on the left wing, but exist symmetrically on the right wing with index R instead of L. The same is true for the drag force, D_R and the winglet forces, L_{W_R} and D_{W_R}, existing symmetrically on the left side. F_L is the force due to elevon deflection over surface area S_a, and F_{L_T} is the force due to elevon deflection over

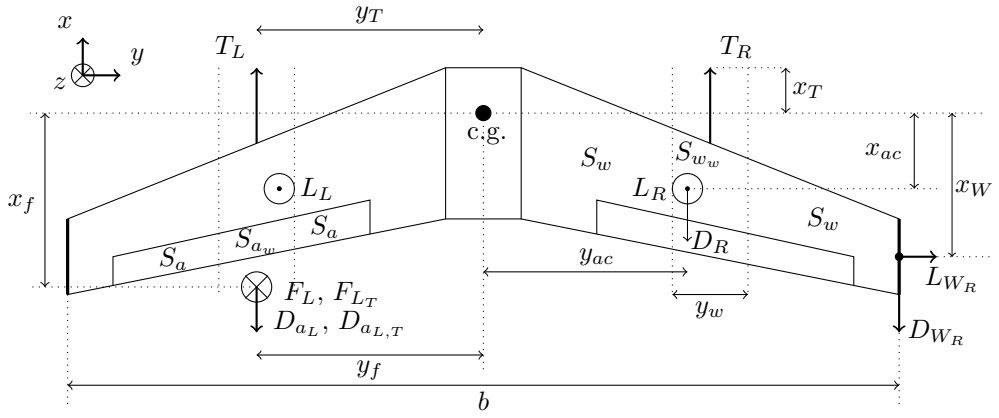

Figure 1: Drawing of the EcoSoar, its propellers with wake and its control surfaces in body frame.

S_{a_w}; the surface in the wake of the propeller. Similarly for the drag, D_{α_L}, $D_{\alpha_{L,T}}$, forces. We also split the wing area into two sections: S_w for the wing area outside the wake, and S_{w_w} for the wing area in the wake. The thrust forces, T_i, are assumed to act at the arrow end of the vector due to the offset in x created by the motor and drive shaft. The lift forces, L_L and L_R, are functions of airflow over wing outside of wake and in the wake, which in turn are functions of aircraft velocity, propeller speed, angle of attack, air density, wing shape, etc.

5.2.1 Aerodynamic Lift force

The lift force of a wing depends on several factors. Mainly: geometrical shape, dynamic pressure and angle of attack. The bigger the wing the more lift. The faster air flows the more lift. The further away from hitting the wing straight on, usually more lift.

Important note: Lift is defined as the **Aerodynamic force component perpendicular to the incoming airflow.** This means that, for example, the lift force labeled in figure 1 as L_L **is not the aerodynamic lift but rather the lift force in body frame.** The same argument applies to the drag forces.

Aerodynamic lift is usually modeled as[3]:

$$L = QC_L S \tag{7}$$

where S is a reference surface area of the wing and Q is the dynamic pressure:

$$Q = \frac{1}{2}\rho v^2 \tag{8}$$

ρ is the density of air and v the velocity of the air hitting the wing. C_L is the coefficient of lift, a function of the angle of attack. This coefficient is not linear. Empirical studies[5] have found functions similair to the one in figure 2.

The angle of attack, α, is formally the angle at which the air is hitting the wing relative the body frame x-z axis. If air is aligned with the x-axis α is zero, and if aligned with the z-axis α is 90. (The airflow will obviously be in the negative axis direction since the airplane is flying in the positive direction and hitting the air). Thus, if we assume no wind the angle of attack is only dependent on the aircraft velocity $\bar{v}$. Normally this is modeled as:

$$\alpha = tan^{-1}(\frac{v_z}{v_x}) \tag{9}$$

but in our case the velocity may have any direction in the x-z plane, and is not limited to the right half plane. The polar coordinates for vector $\bar{v}$ in the figure below, figure 3, are:

$$\begin{aligned} v_x &= r\,cos(\alpha) \\ v_y &= r\,sin(\alpha) \\ r &= \sqrt{v_x^2 + v_z^2} \end{aligned} \tag{10}$$

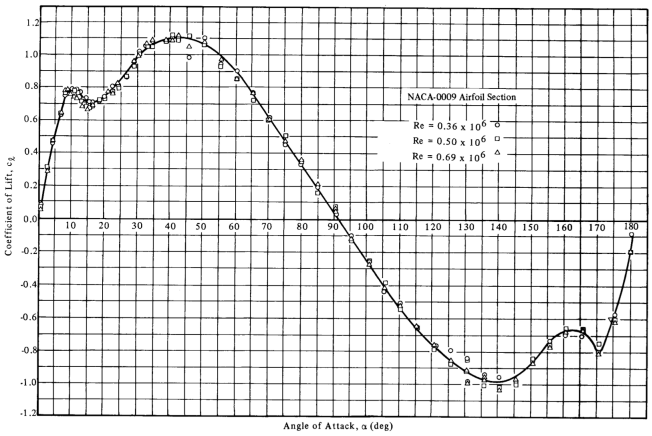

Figure 2: Coefficient of lift for a symmetrical wing vs angle of attack for the entire 180 degree rotation of the wing. The function is periodic.

where α is in the interval $[-\pi, \pi]$.

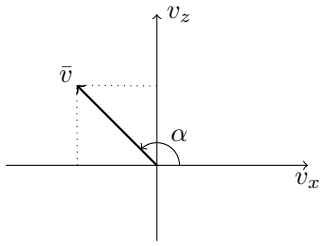

Figure 3: Velocity vector $\bar{v}$ in polar coordinates.

5.2.2 Aerodynamic drag

Similarly to aerodynamic lift the wing will also have an aerodynamic drag force, but parallel to the incoming flow and not perpendicular as lift. The drag is also modeled like so:

$$D = QC_D S \tag{11}$$

where the coefficient of drag, C_D, can also be experimentally obtained as in figure 4.

5.2.3 Lift and drag in body frame

Since the aerodynamic lift and drag forces are relative the incoming airflow, i.e. functions of the angle of attack, α, the body frame Lift and Drag have to transformed:

$$\begin{aligned} L_i &= cos(\alpha)L + sin(\alpha)D \\ D_i &= -sin(\alpha)L + cos(\alpha)D \end{aligned} \tag{12}$$

Note that the above forces are in the direction labeled in figure 1 and not necessarily in the positive axis they act in. From equation 10 we see that

$$\begin{aligned} v_x &= r\, cos(\alpha) \Rightarrow cos(\alpha) = \frac{v_x}{\sqrt{v_x^2 + v_z^2}} \\ v_z &= r\, sin(\alpha) \Rightarrow sin(\alpha) = \frac{v_z}{\sqrt{v_x^2 + v_z^2}} \end{aligned} \tag{13}$$

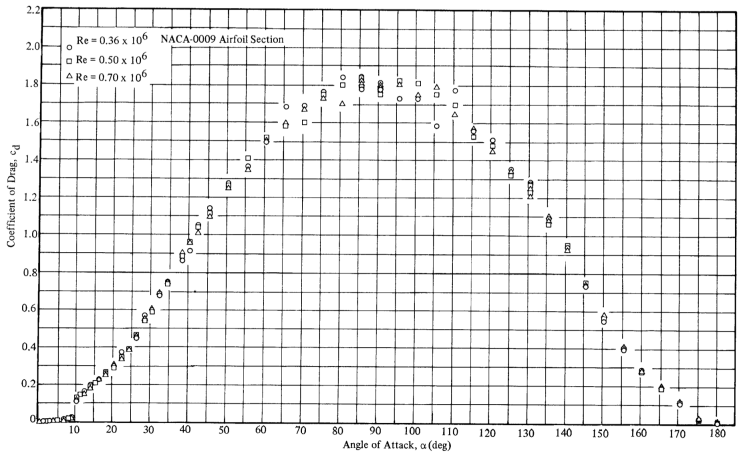

Figure 18. Full Range Section Drag Coefficients for the NACA-0009 Airfoil at Reynolds Numbers of 0.36 x 10^6, 0.50 x 10^6, and 0.69 x 10^6

Figure 4: Coefficient of drag for a symmetrical wing vs angle of attack for the entire 180 degree rotation of the wing.

If we substitute in expressions for aerodynamic lift and drag we obtain:

$$\begin{aligned} L_i =& \frac{v_x}{\sqrt{v_x^2+v_z^2}} QC_L S + \frac{v_z}{\sqrt{v_x^2+v_z^2}} QC_D S \\ D_i =& -\frac{v_z}{\sqrt{v_x^2+v_z^2}} QC_L S + \frac{v_x}{\sqrt{v_x^2+v_z^2}} QC_D S \end{aligned} \tag{14}$$

which simplify into:

$$\begin{aligned} L_i =& S\frac{1}{2}\rho v^2 \left(\frac{C_L v_x + C_D v_z}{\sqrt{v_x^2+v_z^2}} \right) \\ D_i =& S\frac{1}{2}\rho v^2 \left(\frac{-C_L v_z + C_D v_x}{\sqrt{v_x^2+v_z^2}} \right) \end{aligned} \tag{15}$$

where $v = \sqrt{v_x^2+v_y^2+v_z^2}$.

5.3 Moment due to force

Any force not acting at the center of gravity will produce a moment around c.g. The moment of a force is:

$$\bar{M} = \bar{r} \times \bar{F} \tag{16}$$

With our assumptions the above equation can be written as:

$$\bar{M} = (r_x, r_y, 0) \times (F_x, F_y, F_z) = \begin{bmatrix} F_z r_y \\ -F_z r_x \\ F_y r_x - F_x r_y \end{bmatrix} \tag{17}$$

5.3.1 Pitching moment

Lift due to camber on a wing acts at 50% of the cord line. Lift due to angle of attack acts at roughly 25% of the cord line. This makes the force acting point, center of pressure, move along the cord line when angle of attack and aircraft velocity changes. A common simplification is to choose the aerodynamic center, a.c., as the point at which Lift acts. It can be shown that placing the a.c. at the 25% cord position makes the moment generated vary little as angle of attack changes,

yielding simpler equations. The pitching moment due to lift can now be expressed as:

$$\tau_{y,lift} = \sum_{j \in [w, w_w]} C_{m,y,l} Q S_j l + \cancelto{0}{\sum_{j \in [w, w_w]} C_{m,y,l,\alpha} Q S_j l \alpha} \tag{18}$$

where l is the characteristic length of the wing, usually taken as the mean cord for pitching moments and the wingspan for rolling and yawing moments.

5.4 Equations of motion

The equations of motion can be split into three parts: one part due to gravity, one part due to the rigid body frame being an accelerated reference frame, and one part due to aerodynamic forces.

5.4.1 Attitude

The attitude is represented by a quaternion:

$$\bar{q} = [q_0, q_1, q_2, q_3]^T \tag{19}$$

Any vector, $\bar{r}_w$, in world frame can be represented in the body frame by the conversion:

$$\bar{r}_b = \bar{q} \bar{r}_w \bar{q^*} \tag{20}$$

5.4.2 Gravity

In the case of gravity, $\begin{bmatrix} 0 \\ 0 \\ mg \end{bmatrix}_w$, the force, $m\bar{g}$, becomes

$$m\dot{\bar{v}}_b = \begin{bmatrix} 2(\bar{q_1}\bar{q_3} + \bar{q_0}\bar{q_2}) \\ 2(\bar{q_2}\bar{q_3} - \bar{q_0}\bar{q_1}) \\ (\bar{q_0}^2 - \bar{q_1}^2 - \bar{q_2}^2 + \bar{q_3}^2) \end{bmatrix} mg \tag{21}$$

Gravity acts in the center of gravity and creates no moment. Since gravity is in world frame and we want to express it in body frame we need to conjugate the quaternion.

5.4.3 Forces and moments due to accelerated body reference frame

In the case of a rigid body with inertia matrix I, velocity $\bar{v}$ and angular velocity $\bar{\omega}$ relative a fixed frame we have the moment equation:

$$I\dot{\bar{\omega}} = \bar{\tau} - \bar{\omega} \times I\bar{\omega} \tag{22}$$

where τ is the external torque acting on the body.

Similarly, if we include the coriolis force we obtain the forces in our body frame:

$$\bar{F} = \bar{F}_e + 2m\,\bar{\omega} \times \bar{v} \tag{23}$$

where $\bar{F_e}$ is the external forces acting on the body. No other inertial forces are of interest; the linear accelleration is irrelevant since we are not flying inside a linearly accellerating frame, and the other two depend on rotation around a non principal axis.

In our case, with assumptions made, the above equations simplify to:

$$\begin{bmatrix} \dot{\bar{v}} \\ \dot{\bar{\omega}} \end{bmatrix} = \begin{bmatrix} \dot{v_x} \\ \dot{v_y} \\ \dot{v_z} \\ \dot{\omega_x} \\ \dot{\omega_y} \\ \dot{\omega_z} \end{bmatrix} = - \begin{bmatrix} 2(v_z\omega_y - v_y\omega_z) \\ 2(v_x\omega_z - v_z\omega_x) \\ 2(v_y\omega_x - v_x\omega_y) \\ \frac{1}{I_x}(I_z - I_y)\omega_y\omega_z \\ \frac{1}{I_y}(I_x - I_z)\omega_x\omega_z \\ \frac{1}{I_z}(I_y - I_x)\omega_x\omega_y \end{bmatrix} + \texttt{external forces and moments} \tag{24}$$

5.4.4 elevons

Elevon forces are modeled similarly to lift, as well, but with an extra term, δ_i, for the deflection degree in radians:

$$F_i = C_{L_\delta} \sum_{j \in [a, a_w]} Q_{j,i} S_j \delta_i \tag{25}$$

and similairly the drag created by the elevons:

$$D_{\alpha_i} = C_{D_\delta} \sum_{j \in [a, a_w]} Q_{j,i} S_j \delta_i \tag{26}$$

The elevon lift, and drag, coefficient is assumed to be static over all angle of attacks since they will be in the wake of the wing, and the lift and drag are linear in the region of angles the ailerons can deflect.

5.5 Winglets, forces and moments due to sideslip

The aircraft considered here has no tail nor real body. The only surfaces providing relevant forces due to sideslip are the winglets.

The winglets each have an area S_W and are flat plate wings which will generate aerodynamic lift and drag forces due to β providing an angle of attack in their reference frame.

β can be, similarly to α, be expressed in polar coordinates:

$$\begin{aligned} v_x &= r\, cos(\beta) \\ v_y &= r\, sin(\beta) \\ r &= \sqrt{v_x^2 + v_y^2} \end{aligned} \tag{27}$$

The aerodynamic forces, L_β and D_β, from the winglets convert into body forces, directed as in figure 1, similarly to lift and drag from the main wings:

$$\begin{aligned} L_{W_i} &= cos(\beta) L_\beta + sin(\beta) D_\beta \\ D_{W_i} &= -sin(\beta) L_\beta + cos(\beta) D_\beta \end{aligned} \tag{28}$$

where

$$\begin{aligned} L_\beta &= Q C_{L_\beta} S_W \\ D_\beta &= Q C_{D_\beta} S_W \end{aligned} \tag{29}$$

and C_{k_β} are the lift and drag coefficients for each winglet, here assumed to be flat plates. v_z can be assumed to be negligible in the following equations since it will have no measurable effect on the winglets. If we assume v_z to be negligible then the equations simplify into

$$\begin{aligned} L_{W_i} &= \frac{\rho v S_W}{2} \left(C_{L_\beta} v_x + v_y C_{D_\beta} \right) \\ D_{W_i} &= \frac{\rho v S_W}{2} \left(-v_y C_{L_\beta} + v_x C_{D_\beta} \right) \end{aligned} \tag{30}$$

If the sideslip angle, β, is small (which implies v_y small) the lift/drag coefficients can be approximated as

$$\begin{aligned} C_{L_\beta} &\approx \frac{dC_{L_\beta}}{d\beta}\Big|_{\beta=0} \beta \\ C_{D_\beta} &\approx 0 \end{aligned} \tag{31}$$

which results in:

$$\begin{aligned} L_{W_i} &\approx \frac{\rho v S_W}{2} \frac{dC_{L_\beta}}{d\beta}\Big|_{\beta=0} \beta\, v_x \\ D_{W_i} &\approx 0 \end{aligned} \tag{32}$$

This gives us, in body frame, one restoring force from each winglet roughly proportional to the forward velocity squared of the aircraft and the sideslip angle.. The forces have the same magnitude and direction on both sides of the aircraft.

5.5.1 Restoring moment

D_{W_i} are symmetrical on both sides and only create an acceleration in y. They do not generate any moment. L_{W_i}, however, act asymmetrically around c.g. and do generate a moment/torque (note that the force L_{W_R} generates a negative torque around z in our coordinate system):

$$M_z = L_{W_L} x_W + L_{W_R} x_R = -\rho v S_W \frac{dC_{L_\beta}}{d\beta}\Big|_{\beta=0} \beta \, v_x x_W \tag{33}$$

5.5.2 Non linear Forces and Moments

If we do not make the assumption that β is small we instead get the equations:

$$\begin{aligned} M_z =& - x_W \rho v S_W \left(C_{L_\beta}(\beta) v_x + v_y C_{D_\beta}(\beta)\right) \\ D_W =& \rho v S_W \left(-v_y C_{L_\beta}(\beta) + v_x C_{D_\beta}(\beta)\right) \end{aligned} \tag{34}$$

where $D_W = D_{W_L} + D_{W_R}$, and the coefficients of lift and drag are as shown in the figures above, but functions of β instead of α as β becomes the effective angle of attack in the winglets reference frame.

5.5.3 Rolling moment due to sideslip

The center of the winglet is slightly offset in the z-direction from the c.g. by distance z_W. Given the forces L_{W_i} the rolling moment due to sideslip, M_x, is simply

$$M_x = z_W (L_{W_L} + L_{W_R}) \tag{35}$$

5.6 Propeller Thrust

Thrust will be modeled as

$$T_i = K_T \omega_i^2 \tag{36}$$

where K_T is the thrust coefficient of the propeller and ω_i the rotational speed of the propeller.

Behind the propellers an area of airflow is generated, called a wake. Given a propeller diameter of d_P, pushing air through at a rate of v_w the volume of air being moved by the propeller during time t is:

$$V_{air} = \int_0^t \frac{d}{2} \pi^2 v_w dt \,. \tag{37}$$

The air has density ρ converting the volume into mass:

$$m_{air} = \rho \, m_{air} \tag{38}$$

If we assume the air to be stationary in front of the propeller and the aircraft standing still the change in momentum in the air is:

$$\Delta p = m_{air} v_{air} = \rho \frac{d\pi^2}{2} v_w^2 t \tag{39}$$

Force due to change in momentum is:

$$Ft = \Delta p \Rightarrow F = \frac{\Delta p}{t} \tag{40}$$

giving us:

$$F = \rho \frac{d\pi^2}{2} v_w^2 \,. \tag{41}$$

The propellers suffer from aerodynamic losses, non linear effect, etc, so normally an efficiency factor is used. TODO: FIND REFERENCE. This results in an equation as:

$$F = K_v v_w^2 \,. \tag{42}$$

If we instead look at the lift generated by the propeller blades we can find the thrust as a function of propeller rotation speed. Assuming the aircraft has no speed and there is no wind we can model the lift from one propeller blade as:

$$L_i = \int_0^{\frac{d}{2}} \frac{\rho}{2}(\omega_i r)^2 C_L(pitch) dr \tag{43}$$

If we also assume a constant pitch along the diameter of the propeller blade the above integral simplifies into:

$$L_i = \frac{\rho d^3}{48} C_L(pitch)\omega_i^2 \tag{44}$$

and thus with n blades we find the total lift, i.e. thrust:

$$T_i = L = \sum_{i \in [1,n]} L_i = nL_i \tag{45}$$

By comparing the equation for thrust due to rotation speed and thrust due to airflow we conclude that:

$$\begin{aligned} K_v v_w^2 =& n\frac{\rho d^3}{48} C_L(pitch)\omega_i^2 \Rightarrow \\ & v_w = b_w \omega_i \end{aligned} \tag{46}$$

and so the assumption that airflow in the wake is proportional to the propeller angular speed holds.

5.7 Restoring moment due to roll rate

If we assume that v_y is negligible then the Lift and Drag forces in body fram simplify into:

$$\begin{aligned} L_i =& S\frac{1}{2}\rho v^2 \left(\frac{C_L v_x + C_D v_z}{\sqrt{v_x^2 + v_z^2}} \right) = S\frac{1}{2}\rho \sqrt{v_x^2 + v_z^2} \left(C_L v_x + C_D v_z \right) \\ D_i =& S\frac{1}{2}\rho v^2 \left(\frac{-C_L v_z + C_D v_x}{\sqrt{v_x^2 + v_z^2}} \right) = S\frac{1}{2}\rho \sqrt{v_x^2 + v_z^2} \left(-C_L v_z + C_D v_x \right) \end{aligned} \tag{47}$$

If the plane is experiencing rolling, a rotation about the x-axis with a rotational speed of ω_x then a restoring moment will be created. This is because the air is resisting the wings motion through the air.

The rotational speed will yield an increased local v_z, $v_{z,l}$, along the wing:

$$v_{z,l} = v_z + \omega_x y \tag{48}$$

where y is the distance away from the body along the wing. The change in velocity changes the angle of attack locally. The local angle of attack is denoted α_l.

Lets consider the full moment as the integral of the full moment across both wings. This way the symmetrical lift forces will cancel and only the rolling moment will remain.

$$\begin{aligned} M_x =& -\int_{-b/2}^{b/2} y dL_i(y) dy \\ =& -\frac{\rho}{2} \int_{-b/2}^{b/2} y c(y) \sqrt{v_x^2 + v_{z,l}^2} \left(C_L v_x + C_D v_{z,l} \right) dy \end{aligned} \tag{49}$$

If we make the crude assumption that $C_L = a * sin(2 * \alpha)$, and the less crude asumption that $C_D = -b * cos(\alpha) + b$, it is still impossible to find the function $M_x(\omega_x)$ for the entire state space. A term:

$$\int_{-b/2}^{b/2} y \sqrt{(v_1 + \omega y)^2 + v_2^2} dy \tag{50}$$

will remain, and one has to assume $\alpha \in [-\pi/2, \pi/2]$, $v_2 \neq 0$ and/or many of the variables always positive, to find the function without the integral.

A simulator can solve the integral numerically but in order to find smooth analytical expressions for the controller approximations have to be made.

It turns out that the four dimensional function for restoring moment due to roll as a function of roll rate ω_x, v_x and v_z is actually quite linear with respect to ω_x. The remaining function can be closely approximated by a two dimensional polynomial in v_x and v_z allowing for a feedback linearized model to be implemented with very little error.

5.8 Restoring moment due to yaw rate

Similarly the restoring moment due to yaw rate can be obtained from the following integral:

$$M_z = \int_{-b/2}^{b/2} y \left(\frac{1}{2} \rho \sqrt{v_{x,l}^2 + v_z^2} \left(-C_L v_z + C_D v_{x,l} \right) \right) c(y) dy \tag{51}$$

where $v_{x,l} = v_x - \omega_z y$.

For the controller some linear approximation has to be found, similarly as to restoring moment due to roll rate.

5.9 Rolling moment due to yaw rate

Due to the change in forward velocity a change in lift is also produced, inducing a rolling moment obtained similarily:

$$M_x = \int_{-b/2}^{b/2} y \left(\frac{1}{2} \rho \sqrt{v_{x,l}^2 + v_z^2} \left(C_L v_{x,l} + C_D v_z \right) \right) c(y) dy \tag{52}$$

where $v_{x,l} = v_x - \omega_z y$.

For the controller some linear approximation has to be found, similarly as to restoring moment due to roll rate.

5.10 Restoring moment due to pitch rate

Due to the absence of a tail this moment will be much smaller than on aircraft with tail. Most of the wing surface area is behind the center of gravity and due to the wing sweep more surface will be at a longer distance from c.g. in x direction. This means that we can approximate the entire wing to be behind the c.g. This aircraft also has a relatively small inertia around the y axis; the aircraft will quickly turn into the wind.

Since we have modeled the lift in such a way that the pitching moment does not vary with angle of attack we can assume here that it is only proportional to the aircraft velocity and ω_y, similarily as in section **??** but with constants instead of coefficients of lift and drag, giving us the following expression directly:

$$M_y = -\omega_y \rho S \sqrt{v_x^2 + v_z^2} C_{D,\omega_y} \frac{x_{\omega_y}^2}{24} = -\omega_y \rho S C_{\omega_y} \sqrt{v_x^2 + v_z^2} \tag{53}$$

where C_{ω_y} is some constant that needs to be approximated experimentally.

5.11 Actuator dynamics

The actuators onboard are not direct term but contain some dynamics. In this thesis they will be modelled as first order systems.

5.11.1 elevon dynamics

Given an input signal u_{δ_i} for elevon i we model the deflection, δ_i, like so:

$$\dot{\delta}_i = K_{\delta_i}(-\delta_i + u_{\delta_i}) \tag{54}$$

5.11.2 Motor dynamics

Given an input signal u_{ω_i} we model the motor dynamics as so:

$$\dot{\omega_i} = K_{\omega_i}(-\omega_i + u_{\omega_i}) \tag{55}$$

5.12 Full equations of motion

We now include all terms to find the full state space equations:

$$\begin{bmatrix} \dot{v_x} \\ \dot{v_y} \\ \dot{v_z} \\ \dot{\omega_x} \\ \dot{\omega_y} \\ \dot{\omega_z} \\ \dot{q_0} \\ \dot{q_1} \\ \dot{q_2} \\ \dot{q_3} \\ \dot{\delta_L} \\ \dot{\delta_R} \\ \dot{\omega_L} \\ \dot{\omega_R} \end{bmatrix} = \begin{bmatrix} 2g(q_1q_3 + q_0q_2) - \sum_i \left(D_i + D_{i,T} + D_{W_i} + D_{\alpha_i} + D_{\alpha_{i,T}}\right) + T_L + T_R \\ 2g(q_2q_3 + q_0q_1) + L_{W_L} + L_{W_R} \\ g(q_0^2 - q_1^2 - q_2^2 + q_3^2) + \sum_i (L_i + F_i + F_{i_T}) \\ f_1/I_x \\ f_2/I_y \\ f_3/I_z \\ \frac{1}{2}(q_1\omega_x + q_2\omega_y + q_3\omega_z) \\ \frac{1}{2}(q_2\omega_z - q_3\omega_y - q_0\omega_x) \\ \frac{1}{2}(q_3\omega_x - q_0\omega_y - q_1\omega_z) \\ \frac{1}{2}(q_1\omega_y - q_2\omega_x - q_0\omega_z) \\ K_{\delta_L}(-\delta_L + u_{\delta_L}) \\ K_{\delta_R}(-\delta_R + u_{\delta_R}) \\ K_{\omega_L}(-\omega_L + u_{\omega_L}) \\ K_{\omega_R}(-\omega_R + u_{\omega_R}) \end{bmatrix} - \begin{bmatrix} 2(v_z\omega_y - v_y\omega_z) \\ 2(v_x\omega_z - v_z\omega_x) \\ 2(v_y\omega_x - v_x\omega_y) \\ \frac{1}{I_x}(I_z - I_y)\omega_y\omega_z \\ \frac{1}{I_y}(I_x - I_z)\omega_x\omega_z \\ \frac{1}{I_z}(I_y - I_x)\omega_x\omega_y \\ 0 \\ 0 \\ 0 \\ 0 \\ 0 \\ 0 \\ 0 \\ 0 \end{bmatrix} \tag{56}$$

where f_1 is given by:

$$\begin{aligned} f_1 =& y_f C_{L_\delta} \sum_{j\in[a,a_W]} S_j \left(Q_{j,L}\delta_L - Q_{j,R}\delta_R\right) \text{ :: diff in ail deflection} \\ &- \frac{\rho}{2}\int_{-b/2}^{b/2} yc(y)\sqrt{v_x^2 + v_{z,l}^2}\left(C_L(\alpha_l)v_x + C_D(\alpha_l)v_{z,l}\right)dy \text{ :: restmom roll} \\ &+ \int_{-b/2}^{b/2} y\left(\frac{\rho}{2}\sqrt{v_{x,l}^2 + v_z^2}\left(C_L v_{x,l} + C_D v_z\right)\right)c(y)dy \text{ :: roll due to yaw rate} \end{aligned} \tag{57}$$

, f_2 by:

$$\begin{aligned} f_2 =& x_f C_{L_\delta}\left(\sum_{j\in[a,a_W]} S_j\left(Q_{j,L}\delta_L + Q_{j,R}\delta_R\right)\right) \text{ :: joint ail deflection} \\ &+ \sum_{j\in[w,w_w]} C_{m,y,l}Q_j S_j l \text{ :: pitch moment} \\ &- \omega_y\rho\, 2S_w C_{\omega_y}\sqrt{v_x^2 + v_z^2} \text{ :: restmom pitch rate} \end{aligned} \tag{58}$$

and f_3 by:

$$\begin{aligned} f_3 =& y_T\left(T_L - T_R\right) \text{ :: diff in T} \\ &- x_W\rho v S_W\left(C_{L_\beta}(\beta)v_x + v_y C_{D_\beta}(\beta)\right) \text{ :: mom due to sideslip} \\ &+ \int_{-b/2}^{b/2} y\left(\frac{\rho}{2}\sqrt{v_{x,l}^2 + v_z^2}\left(-C_L v_z + C_D v_{x,l}\right)\right)c(y)dy \text{ :: restmom yaw rate} \end{aligned} \tag{59}$$

$Q_{j,i}$ is given by $\frac{\rho}{2}v_k^2$ where v_k is the speed in the relevant area, which can be either the aircraft velocity if the surface in question is outside the propeller wake, or the propeller wake air speed given by the left or right propeller speed if inside the propeller wake.

Variables like D_i and $D_{i,T}$ differ by both which area they use and which speed the airflow has since they are separated by if they are on the right or left side, inside or outside the propeller wake, and thus the currect expressions for the airspeed have to be used. The same argument goes for expressions which depend on α.

6 EcoSoar

6.1 CAD model

6.2 modifications to dual engine

6.3 Building

3D printing, building, etc

6.4 Parameter estimation/declarations

7 Robust controller development and Implementation

The controller implemented is based on a non-linear Proportional squared (P^2) controller by Emil Fresk[4]. The controller was first implemented on a simulator of the EcoSoar made in Simulink. A few other controllers were first attempted, among them a Feedback Linearization controller.

7.1 Feedback Linearization

Didn't work.

7.1.1 Mimo: Lie derivatives and brackets

7.1.2 Decoupling matrix

7.2 L1 parameter compensation/estimation

Maybe still needed?

7.3 Simulink

The full non linear state space equations derived above in section 5.12 were put in a matlab function block surrounded by state integrators to generate the full state. Parameters were either measured or estimated to complete the numerical simulator. Controllers could then be tested and evaluated quickly. A instant render of the simulation was also added through Simulinks VR support blocks.

7.4 Pixhawk firmware

Mathworks has support for the embedded coder to directly upload apps into the PX4 NuttX Real Time OS that can run on the Pixhawk 1. The firmware has to be flashed to PX4 on the Pixhawk, files modified on the SD card and a wide range of supporting softwares must be installed on the host computer.

7.5 Initial testing on Bixler

The evaluate the firmware/simulink controller deployment into a Pixhawk a Bixler was used. The Pixhawk was put into the Bixler to replace the receiver inside, necessary hardware added and then a simple FlyByWire controller was implemented and uploaded into the Pixhawk from Simulink. Results were very good, the Bixler flew as expected and no issues with the software on-board.

7.6 P2-controller

The Pixhawk was then removed and placed on a small flying fixed wing with dual rotors to test a simple version of the full controller. The P2 controller [4] was implemented along with separate tuning for the three axis. The flying wing would hover well, but no logs could initially be produced.

7.7 Torque translator

The small flying wing has propeller wakes that covered the entire elevon. The EcoSoar does not. Therefor it is of interest to normalize the actuation signals given the current state so that they produce the requested torque from the P2 controller. By assuming that the airflow inside the wake and outside the wake do not affect each other and that the dynamic pressure is the dominating effect a simple function can be found that takes the current rotational speeds of the propellers, the current velocity of the aircraft and requested torque around x and y axis and gives the deflection angle of the control surfaces.

We assume that damping due to rotational speeds do not exist, winglets have no z-offset, and no net pitch moment is created by the lift from the wings. The equations for torque around each axis then become:

$$\begin{aligned} \tau_x =& y_f(F_L + F_{L_T} - F_{R_T} - F_R) \\ \tau_y =& x_f(F_{L_T} + F_L + F_{R_T} + F_R) \\ \tau_z =& y_T(T_L - T_R) \end{aligned} \tag{60}$$

which indicates that the elevons force per deflection is proportional to the airflow speed over them squared. The P2 controller outputs desired angular acceleration, $\dot{\omega}_i$, not torque. Necessary torque, τ_i, for axis i is given by

$$\tau_i = \dot{\omega}_i I_i \tag{61}$$

Solving for differential thrust is trivial. Taking the inertia around each axis into account the necessary deflection for each elevon, u_{δ_i} can be solved for given the current state:

$$\begin{aligned} u_{\delta_L} =& \frac{-0.5\tau_y}{k_1 sgn(v_x)v^2 + k_2\omega_L^2} - \frac{0.5\tau_x}{k_3 sgn(v_x)v^2 + k_4\omega_L^2} \\ u_{\delta_R} =& \frac{-0.5\tau_y}{k_1 sgn(v_x)v^2 + k_2\omega_R^2} + \frac{0.5\tau_x}{k_3 sgn(vx)v^2 + k_4\omega_R^2} \end{aligned} \tag{62}$$

where $k_{[1-4]}$ are numerical constants given by aircraft parameters.

8 Results

8.1 Performance in Simulations

Since all parameters are well known/set in the simulator and assumptions are the same for the simulator and controller the system works very well in simulation.

8.2 Performance in reality

9 Conclusion

References

[1] Michel Goossens, Frank Mittelbach, and Alexander Samarin. *The LaTeX Companion*. Addison-Wesley, Reading, Massachusetts, 1993.

[2] Albert Einstein. *Zur Elektrodynamik bewegter Körper*. (German) [*On the electrodynamics of moving bodies*]. Annalen der Physik, 322(10):891–921, 1905.

[3] Robert C Nelson *Flight Stability and Automatic Control* [*Second Edition*] ISBN: 0-07-066110-3

[4] Emil Fresk and George Nikolakopoulos *Full Quaternion Based Attitude Control for a Quadrotor* 2013 European Control Conference (ECC) July 17-19, 2013, Zürich, Switzerland. 978-3-033-03962-9/©2013 EUCA

[5] Robert E. Sheldahl, Paul C. Klimes *Aerodynamic CHaracteristics of Seven Symmetrical Airfoil Sections Through 180-Degree Angle of Attack for Use in Aerodynamic Analysis of Vertical Axis Wind Turbines* Sandia National Laboratories - energy report SAND80-2114 Unlimited Release UC-60

[6] Joan Solà *Quaternion kinematics for the error-state KF* February 2, 2016